it is tilted to bring the area of least bowl curvature into contact with the surface. Additionally, as it is possible for two benzene tabs to lie concomitantly over respective fourfold hollow sites, **2** adopts a molecular orientation with two tabs proximal to the surface.

## Results and Discussion

The choice of Cu(100) as surface was motivated by the mobility at room temperature. While the mobility of **2** at room temperature on surfaces such as Au(111) or Ag(111) is too high in order to observe ordered structures, it is sufficiently low on Cu(100). Ordered self-assembly of these molecules is observed at 300 K and at coverages of less than a complete monolayer. From roughly 50% of a full monolayer up to the close-packed monolayer islands of an ordered 2D structure are observed with scanning tunneling microscopy (STM, Fig. 2a). Rotational domains are identified and in each single domain, the molecules are oriented uniformly in lines along the same direction. The relative orientation of different rotational domains is 90° (Fig. 2b), suggesting that the molecules are aligned along the principle axes of the Cu(100) surface.

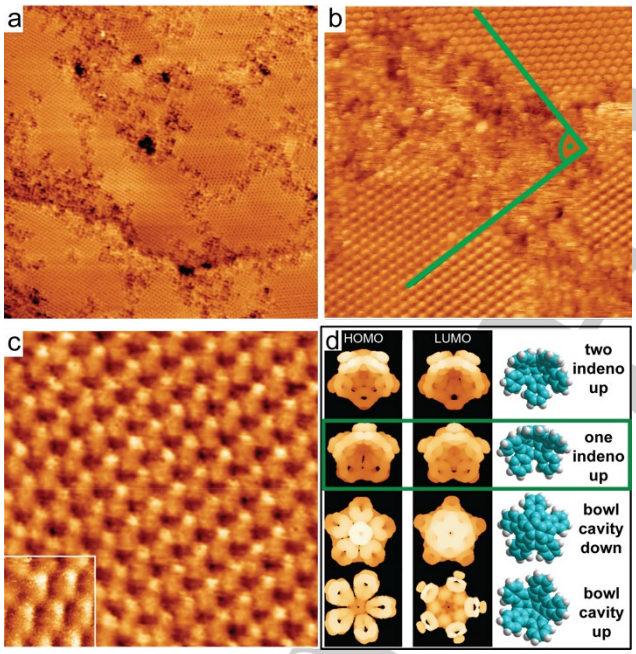


**Figure 2.** STM images of **2** self-assembled on Cu(100) at room temperature. a) Long range STM image (100 nm × 100 nm, 2.62 V, 25 pA) showing ordered areas of **2**, but also empty and disordered areas. b) Rotational domains with lattice vectors that are normal to each other are observed. (29.7 nm × 29.7 nm, 2.6 V, 25 pA). c) STM image showing asymmetric contrast of each molecule (9.3 nm × 9.3 nm, –2.18 V, 25 pA). The inset shows a high-resolution STM image of few molecules (4.8 nm × 4.8 nm, –3.08 V, 26 pA). d) Molecular drawings of the four possible adsorption footprints of **2** and their corresponding electron density maps (cutoff: 0.001 e/Å$^3$) of the frontier orbitals. The green rectangle highlights the contrast that fits best the STM observation.

At higher magnification STM reveals a non-uniform contrast for each molecule: a round lobe with a bright protrusion on one side (Fig. 2c). The STM appearance of frontier orbitals can be easily evaluated by Extended Hückel Theory (EHT). A comparison of their electron density maps for different adsorption configurations allows exclusion of bowl cavity-up and bowl cavity-down configurations (Fig. 2d). A bright off-centered protrusion appearance in STM suggests strongly a tilted configuration. In addition, STM images with sub-molecular resolution show that the bright off-centered protrusion represents rather a single lobe (Fig. 2c). Therefore, the overall contrast of a single molecule agrees better with the electron density map of a molecule adsorbing with two indeno groups proximal to the surface and one indeno group pointing up (Fig. 2d). Note that **3** was found to align with its single indeno group parallel to the surface.[21]

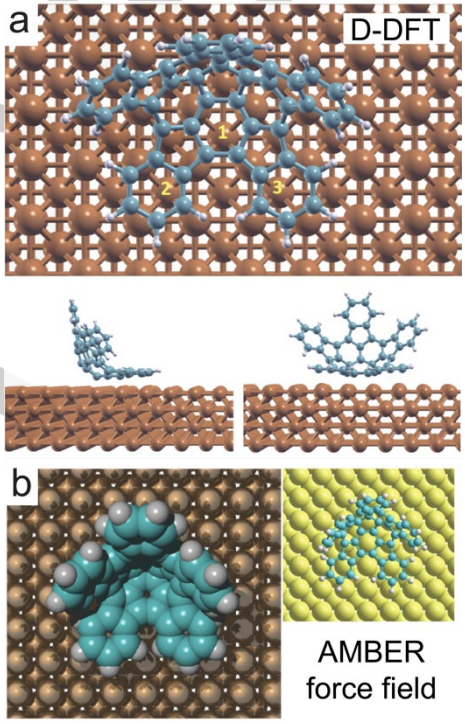


**Figure 3.** Top and side views of relaxed configurations of **2** obtained from D-DFT and force field modelling. a) Relaxed configurations of single **2** adsorbed on a 4-layer slab of Cu(100) according to D-DFT calculations. Hexagonal rings, labeled 1, 2 and 3, of the relaxed molecule are located above hollow sites at a distance of about 2.2 Å to the topmost copper layer. b) Amber force field calculations come to similar conclusions with respect to the molecular alignment, except the C6 rings residing on-top of Cu atoms.

The conclusions on the tilted adsorption configuration from experiment are supported by theoretical considerations based on molecular mechanics (MM) and dispersion-enabled density functional theory (D-DFT, Fig. 3). In both cases – and independent of the chosen initial configurations of the molecule on the surface – the relaxed molecule aligned itself indeed with two indeno groups close to the surface. Although MM has the benzene tabs aligned on-top of Cu surface atoms, it has been shown for pentahelicene on Cu(111), for example, that MM is insufficient for precise determination of the surface binding site.[22] D-DFT predicts that three C6 rings, two of indeno groups and one

of the corannulene core become located above fourfold hollow sites (Fig. 3). This finding agrees with the common observation reported in the literature, that aromatic hydrocarbons adsorb with their C6 ring center preferably above hollow sites on copper surfaces.[23-25]

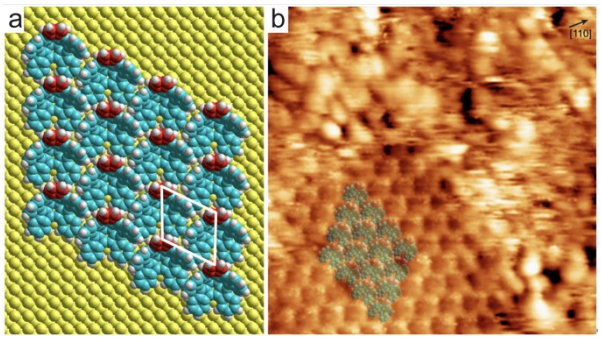


**Figure 4.** a) Structure model for the close-packed 2D lattice of **2** on Cu(100). b) Superposition of model and STM image (15 nm × 15 nm, –3.079V, 26pA).

The equal appearance of molecules of **2** in a single domain suggests identical azimuthal alignment for all of them. Figure 4a shows a structure model for a single domain derived from STM. The superposition of such model onto an island of molecules fits very well to the STM contrast (Fig. 4b). In such relative alignment two indeno groups that are not in contact to the surface point to the convex sides of adjacent molecules, suggesting a non-covalent intermolecular interaction *via* a C-H···π bonding motif. But short distances between different groups of adjacent molecules in lattices are not automatically a confirmation of attractive intermolecular bonding.[26,27] Short distances in 2D surface lattices can also emerge from packing constraints, such as the strong surface interaction mechanism in conjunction with preferred surface binding sites. However, it has been shown for small aggregates, (dimers, trimers, etc.) of fragment buckybowls of $C_{70}$ that intermolecular C-H···π and π···π bonding indeed come into effect on Cu(111).[19,21,28] As this packing motif is observed already at 50% of the complete monolayer, the conclusion on binding mechanism based on relative alignment seems valid.

Table 1 lists structural parameters of the 2D lattice of **2** in comparison with buckybowl **3** on the same surface.[29] The area under a single molecule in Å$^2$ has been calculated by the number of Cu atoms in the unit cell and the area of a Cu(100) unit cell (2.55 Å × 2.55 Å). Although **3** can only bind with one indeno group to the surface, both species form a lattice of identical lateral density. Again, an indication that a particular surface binding site dominates the molecule-surface interaction.

**Table 1.** Structural parameters of the self-assembly of **2** on Cu(100) compared with those of **3** on the same surface.

| Molecule | Monoindenocorannulene $C_{24}H_{12}$, **3** | Pentaindenocorannulene $C_{50}H_{20}$, **2** |
|---|---|---|
| # of indeno groups | 1 | 5 |
| symmetry | $C_{1V}$ | $C_{5V}$ |
| unit cell (matrix notation[a]) | $\begin{pmatrix} 4 & 0 \\ -1 & 4 \end{pmatrix}$ | $\begin{pmatrix} 4 & 0 \\ -2 & 4 \end{pmatrix}$ |
| area per molecule [Å$^2$/molec.] | 104 | 104 |

[a] According to ref. [30].

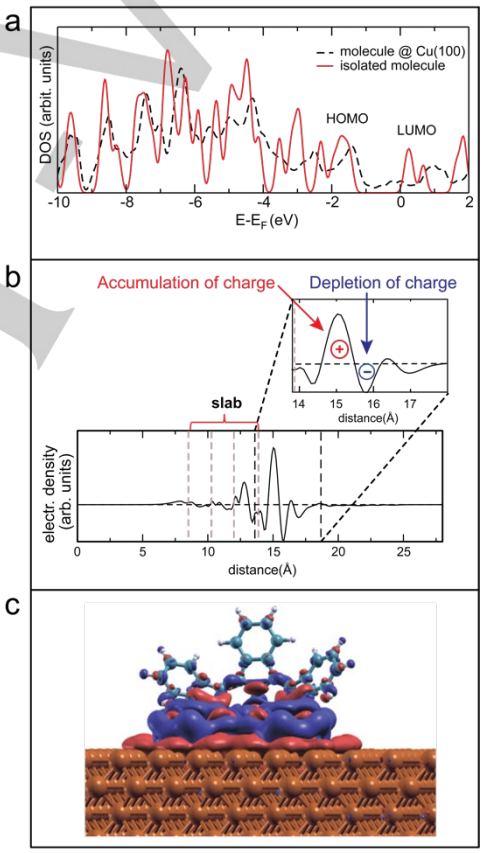


**Figure 5.** Projected density of states (PDOS) and charge distribution throughout the adsorbate. a) PDOS projected on the isolated molecule (red curve) and onto the molecule adsorbed on the slab (black dashed curve). For the adsorbate HOMO is fully occupied and LUMO is not occupied. Consequently, there is no charge transfer ($E–E_F = 0$ is the Fermi energy level). b) Planar averaged charge density difference between total adsorbate complex and the two separate fragments as function of position perpendicular to the slab, plotted through the entire interface. The lower part of the molecule shows a depletion, while charge is accumulated between the molecule and the topmost Cu atom layer. c) 3D charge density difference between the entire complex and the two separate fragments (contour cutoff value of $8 \cdot 10^{-4}$ e/Å$^3$, blue color indicates depletion of charge, red color indicates accumulation of charge).

One important aspect of the adsorptive bond of buckybowls to metal surfaces is Pauli repulsion. Due to the high electron density at the convex bowl side, buckybowls exhibit a large intrinsic dipole moment, that turns into a substantial interface dipole moment at the metal surface by pushing the metal electrons back into the substrate.[13] With the electron density largest above the center pentagonal ring at the convex side, the Pauli repulsion in the substrate would be too substantial for an adsorbate configuration with the fivefold axis perpendicular to the surface. Consequently, the tilt of **2** as adsorbate can be characterized by minimizing Pauli repulsion plus maximizing the vdW contact area. However, Pauli repulsion for **2** on Cu(100) in the tilted adsorbate mode is still substantial.

DFT calculations show that there is no charge transfer between the molecule and the copper surface (Fig. 5a). However, there is a pronounced charge redistribution at the interface due to Pauli repulsion. The charge density plot perpendicular to the surface shows a charge depletion in the molecular region and accumulation of charge underneath the molecule (Fig. 5b), resulting in an interface dipole moment of 7.4 Debye for the single adsorbate. The induced interface dipole is directed opposite to the intrinsic surface dipole based on the spill-out of electrons at the clean metal surface and decreases the surface work-function. Qualitatively, the charge density plot reflects also the dipole-dipole interaction character due to mirror charge established in the substrate. A depletion in the molecule at 17 Å causes a mirror charge (accumulation) at 13 Å, for example (Fig. 5b). Similar values have been reported (theoretically and experimentally) for **1**, pentamethyl-**1** and **3** on Cu(111).[13,21] The polarization binding mechanism of adsorption has previously been described for benzene on coinage metals.[31] Although two indeno arms parallel to the surface suggest maximizing vdW contact, it is either the Pauli repulsion or the fact that three hollow sites provide the strongest binding that dominates the adsorption mechanism of **2**. The D-DFT calculations yield a strong binding of 5.7 eV for **2**, which is substantially larger than calculated for **3**.[21] D-DFT calculations for **3** on Cu(111) also showed that the single indeno group was not perfectly parallel located to the surface plane, indicating a binding to the surface rather at the bowl and not by maximal vdW contact to the surface *via* the benzene indeno tab.[21]

## Conclusions

Self-assembly of fivefold symmetric objects is usually less favorable than with other symmetries because of the incompatibility of these fivefold symmetric structures with all 17 crystallographic plane groups. Therefore, if no steric hindrance is built within the molecule, fivefold symmetry is usually avoided, for example by interdigitation or by a substantial tilt of the molecule. This is indeed the case here for **2** on Cu(100). Neither convex nor concave binding of **2** with the fivefold axis normal to the substrate plane would allow for substantial vdW contact area between **2** and the substrate surface.

With such strong binding of **2** to the surface it is unlikely that maximization of vdW contact plays a dominant role. Rather occupation of favored binding sites, that is, three benzoid rings over fourfold hollow sites, in combination with minimizing Pauli repulsion cause **2** to be aligned with two indeno groups parallel to the surface. Hence, a consistent picture of polynuclear aromatic hydrocarbons binding to metal surfaces is developing in which surface area and benzenoid-ring disposition play an important role in the nature of binding. There is a reasonable expectation that these rules will hold in general for carbon rich non-planar graphenoids, such as fullerene fragments or helicenes.[32,33] Molecular tiles with geometrically orthogonal segments offer a control mechanism in which the segment best suited to optimize the surface coverage will bind flat and its orthogonal segment will extend normal to the surface plane. The shape recognition of the surface-binding portion should result in tilings with regular spaced features like gratings or boxes.

## Experimental Section

*Experimental Details*

Pentaindenocorannulene (**2**) was synthesized as reported previously.[34] The Cu(100) single crystal surface (MaTecK, Jülich) was cleaned by cycles of argon ion sputtering and subsequent annealing to 700 K for 2 minutes. **2** was sublimed at 593 K in *vacuo* from a crucible onto the Cu(100) surface held at room temperature during deposition. STM (Omicron Nanotechnology GmbH, SCALA PRO 4.1 software) images were acquired in constant current mode a room temperature.

*Theoretical Methods*

For molecular modelling, single molecules were prepared with Amber force field of Hyperchem 8.0. A four-layer Cu(111) slab with periodic boundary conditions was used as template, with the copper atoms fixed in space during the calculations. EHT was performed in HyperChem 8.0 directly on a force field-optimized structure. The charge density contours of the frontier orbitals were displayed using Igor (code by Dr. Oliver Gröning, Empa). DFT calculations were performed with an optB86-vdW functional,[35,36] which accounts for dispersion effects, and ultrasoft pseudopotentials as implemented in the Quantum Espresso package (http://www.quantum-espresso.org/). The single-particle electronic wave functions and charge densities were expanded in a plane-wave basis set, up to an energy cutoff of 25 Ry and 250 Ry, respectively. An isolated molecule on the surface was considered, where a periodic four-atom-layer slab consisting of 440 Cu atoms and a vacuum space of 23 Å perpendicular to the surface direction was used. Dipole corrections along the direction perpendicular to the metal surface area were applied. Structural relaxations have been performed at the GAMMA point with the bottom two layers fixed and all other atoms allowed to relax unconstrained until the forces on each atom are less than 0.013 eV /Å.

## Acknowledgements

The research described in this paper has been supported by the Swiss National Science Foundation (Grants 152559 and 163296), and the UZH Priority Program LightChEC. KKB and JSS thank the National Basic Research Program of China (2015CB856500), the Qian Ren Scholar Program of China, and the Synergetic

Innovation Center of Chemical Science and Engineering (Tianjin) for supporting this work.

**Keywords:** buckybowls • scanning tunneling microscopy • dispersion-enabled density functional theory • metal surfaces • 2D self-assembly

[1] a) Y.-T. Wu, J. S. Siegel, *Chem. Rev.* **2006**, *106*, 4843–4867. b) V. M. Tsefrikas, L. T. Scott, *Chem. Rev.* **2006**, *106*, 4868–4884.

[2] G. Valenti, C. Bruno, S. Rapino, A. Fiorani, E. A. Jackson, L. T. Scott, F. Paolucci, M. Marcaccio, *J. Phys. Chem. C* **2010**, *114*, 19467–19472.

[3] T. Bauert, L. Merz, D. Bandera, M. Parschau, J. S. Siegel, K.-H. Ernst, J. *Am. Chem. Soc.* **2009**, *131*, 3460–3461.

[4] Q. Stöckl, D. Bandera, C. S. Kaplan, K.-H. Ernst, J. S. Siegel, *J. Am. Chem. Soc.* **2014**, *136*, 606–609.

[5] L. Zoppi, T. Bauert, J. S. Siegel, K. K. Baldridge, K. H. Ernst, *Phys. Chem. Chem. Phys.* **2012**, *14*, 13365–13369.

[6] W. Xiao, D. Passerone, P. Ruffieux, K. Aït Mansour, O. Gröning, E. Tosatti, J. S. Siegel, R. Fasel, *J. Am. Chem. Soc.* **2008**, *130*, 4767–4771.

[7] T. Bauert, K. K. Baldridge, J. S. Siegel, K.-H. Ernst, *Chem. Comm.* **2011**, *47*, 7995–7997.

[8] A. Baby, H. Lin, A. Ravikumar, C. Bittencourt, H. A. Wegner, L. Floreano, A. Goldoni, G. Fratesi, *J. Phys. Chem. C* **2018**, *122*, 10365–10376.

[9] B. Calmettes, S. Nagarajan, A. Gourdon, Y. Benjalal, X. Bouju, M. Abel, L. Porte, R. Coratger, *J. Phys. Chem. C* **2009**, *113*, 21169–21176.

[10] O. Guillermet, E. Niemi, S. Nagarajan, X. Bouju, D. Martrou, A. Gourdon, S. Gauthier, *Angew. Chem. Int. Ed.* **2009**, *48*, 1970–1973.

[11] L. Merz, M. Parschau, L. Zoppi, K. K. Baldridge, J. S. Siegel, K.-H. Ernst, *Angew. Chem. Int. Ed.* **2009**, *48*, 1966–1969.

[12] L. Merz, T. Bauert, M. Parschau, G. Koller, J. S. Siegel, K.-H. Ernst, *Chem. Commun. (Camb.)* **2009**, 5871–5873.

[13] T. Bauert, L. Zoppi, G. Koller, A. Garcia, K. K. Baldridge, K.-H. Ernst, *J. Phys. Chem. Lett.* **2011**, *2*, 2805–2809.

[14] T. Bauert, L. Zoppi, G. Koller, J. S. Siegel, K. K. Baldridge, K.-H. Ernst, *J. Am. Chem. Soc.* **2013**, *135*, 12857–12860.

[15] I. Aprahamian, D. Eisenberg, R. E. Hoffman, T. Sternfeld, Y. Matsuo, E. A. Jackson, E. Nakamura, L. T. Scott, T. Sheradsky, M. Rabinovitz, *J. Am. Chem. Soc.* **2005**, *127*, 9581–9587.

[16] A. Ayalon, A. Sygula, P. C. Cheng, M. Rabinovitz, P. W. Rabideau, L. T. Scott, *Science* **1994**, *265*, 1065–1067.

[17] W. Xiao, K.-H. Ernst, K. Palotás, Y. Zhang, E. Bruyer, L. Peng, T. Greber, W. A. Hofer, L. T. Scott, R. Fasel, *Nat. Chem.* **2016**, *8*, 326–330.

[18] M. Parschau, R. Fasel, K.-H. Ernst, O. Gröning, L. Brandenberger, R. Schillinger, T. Greber, A. P. Seitsonen, Y.-T. Wu, J. S. Siegel, *Angew. Chem. Int. Ed.* **2007**, *46*, 8258–8261.

[19] Q. S. Stöckl, T.-C. Wu, A. Mairena, Y.-T. Wu, K.-H. Ernst, *Faraday Discuss.* **2017**, *204*, 429–437.

[20] T. Schilling, S. Pronk, B. Mulder, D. Frenkel, *Phys. Rev. E* **2005**, *71*, 036138/1–6.

[21] L. Zoppi, Q. Stöckl, A. Mairena, O. Allemann, J. S. Siegel, K. K. Baldridge, K.-H. Ernst, *J. Phys. Chem. B* **2017**, *122*, 871–877.

[22] A. Mairena, L. Zoppi, J. Seibel, A. F. Tröster, K. Grenader, M. Parschau, A. Terfort, K.-H. Ernst, *ACS Nano* **2017**, *11*, 865–871.

[23] K. Toyoda, Y. Nakano, I. Hamada, K. Lee, S. Yanagisawa, Y. Morikawa, *J. Electron Spectrosc. Relat. Phenom.* **2009**, *174*, 78–84.

[24] J. A. Larsson, S. Elliott, J. Greer, J. Repp, G. Meyer, R. Allenspach, *Phys. Rev. B* **2008**, *77*, 115434/1-9.

[25] J. A. Smerdon, M. Bode, N. P. Guisinger, J. R. Guest, *Phys. Rev. B* **2011**, *84*, 165436/1–7.

[26] J. D. Dunitz, A. Gavezzotti, *Angew. Chem. Int. Ed.* **2005**, *44*, 1766–1787.

[27] J. D. Dunitz, *IUCrJ* **2015**, *2*, 157–158.

[28] Q. S. Stöckl, Y.-C. Hsieh, A. Mairena, Y.-T. Wu, K.-H. Ernst, *J. Am. Chem. Soc.* **2016**, *138*, 6111–6114.

[29] Q. S. Stöckl, PhD thesis; University of Zürich, 2014.

[30] L. Merz, K.-H. Ernst, *Surf. Sci.* **2010**, *604*, 1049–1054.

[31] a) G. Witte, S. Lukas, P. S. Bagus, C. Wöll, *Appl. Phys. Lett.* **2005**, *87*, 263502/1-3. b) P. S. Bagus, K. Hermann, C. Wöll, *J. Chem. Phys.* **2005**, *123*, 184109. c) R. Caputo, B. P. Prascher, V. Staemmler, P. S. Bagus, C. Wöll, C, J. *Phys. Chem. A* **2007**, *111*, 12778−12784.

[32] K.-H. Ernst, *Acc. Chem. Res.* **2016**, *49*, 1182–1190.

[33] A. K. Dutta, A. Linden, L. Zoppi, K. K. Baldridge, J. S. Siegel, *Angew. Chem. Int. Ed.* **2015**, *54*, 10792–10796.

[34] S. Lampart, L. M. Roch, A. K. Dutta, Y. Wang, R. Warshamanage, A. D. Finke, A. Linden, K. K. Baldridge, J. S. Siegel, *Angew. Chem. Int. Ed.* **2016**, *55*, 14648–14652.

[35] J. Klimeš, D. R. Bowler, A. Michaelides, *Phys. Rev. B* **2011**, *83*, 195131/1–13.

[36] J. Carrasco, W. Liu, A. Michaelides, A. Tkatchenko, *J. Chem. Phys.* **2014**, *140*, 084704.

# FULL PAPER

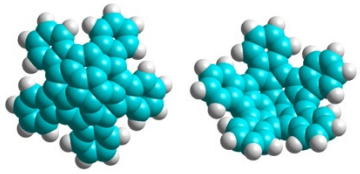

**Bowl dance:** The buckybowl pentaindenocorannulene orients itself on a copper surface such that two arms are aligned parallel to the surface, thus maximizing van der Waals contact. However, theoretical evaluations suggest that this adsorbate motif originates from binding of aromatic C6 rings to surface hollow sites plus minimizing Pauli repulsion. An unidirectional alignment of the molecules in extended 2D domains suggests rim C-H bonding to convex bowl side $\pi$ states.

A. Mairena, L. Zoppi, S. Lampart, K. K. Baldridge, J. S. Siegel, K.-H. Ernst*

***Page No. – Page No.***

**Fivefold Symmetry and 2D Crystallization: Self-Assembly of the Buckybowl Pentaindenocorannulene on a Cu(100) Surface**